Polymer 49 (2008) 5643–5649

Contents lists available at ScienceDirect

Polymer

journal homepage: www.elsevier.com/locate/polymer

A novel conjugated polymer based on cyclopenta[*def*]phenanthrene backbone with spiro group

Suhee Song [a], Youngeup Jin [a], Jinwoo Kim [a], Sung Heum Park [b], Sun Hee Kim [b], Kwanghee Lee [b], Hongsuk Suh [a,]*

[a] *Department of Chemistry and Chemistry Institute for Functional Materials, Pusan National University, 30 Jangjeon-dong, Geumjeong-gu, Busan 609-735, Republic of Korea*
[b] *Department of Materials Science and Engineering, Gwangju Institute of Science and Technology, Gwangju 500-712, Republic of Korea*

ARTICLE INFO

Article history:
Received 16 July 2008
Received in revised form 4 October 2008
Accepted 8 October 2008
Available online 21 October 2008

Keywords:
Light-emitting diodes
Electroluminescence
Cyclopentaphenanthrene

ABSTRACT

Poly(2,6-(4,4-bis(2-ethylhexyl)-4*H*-cyclopenta[*def*]phenanthrene)) (PCPP) is a stable blue light emitting conjugated polymer even after annealing at 150 °C or operation of the device in air. The spiro form of PCPP, poly(2,6-(3′,6′-bis(2-ethylhexyloxy)-4,4′-spirobi(4*H*-cyclopenta[*def*]phenanthrene))) (spiro-PCPP), has been synthesized by Yamamoto polymerization. The PL emission spectrum of the polymer in THF solution shows a maximum peak at 398 nm, nearly identical with that of PCPP. The PL spectrum of the polymer in the solid state exhibits a maximum peak at 451 nm, which is red-shifted over 50 nm from that of the solution, due to the inter-chain interaction of the polymers. The PL spectra of spiro-PCPP in the mixture of THF and MeOH from 9:1 to 3:7 ratios showed increasing peaks at 458 and 484 nm. With an increased ratio of the hydrophilic solvent (MeOH), the inter-chain interaction of the hydrophobic polymers was enhanced to show peaks at 458 and 484 nm. This phenomenon has the same tendency as compared to the PL spectrum in solid thin film state. The polymer LED with the configuration of ITO/PEDOT/spiro-PCPP/Ca:Al emitted light with maximum peaks at around 463 nm. The emission color of the spiro-PCPP device is sky blue with the CIE coordinates of (0.14, 0.15), which are close to those of the standard blue (0.14, 0.08).

1. Introduction

Because of the potential application as large-area light-emitting diodes (LEDs), various kinds of conjugated polymers have been developed for polymer light-emitting diodes (PLEDs) [1,2]. Many conjugated polymers, including the polyfluorenes (PFs), [3,4] polycyclopentaphenanthrene [5,6] and poly(phenanthrene) [7,8] for blue [9] and poly(*p*-phenylenevinylene) (PPVs) [10,11] for green [12] or red [13], have obtained much attention due to their thermal and chemical stability and exceptionally high solution and solid-state fluorescence quantum yield.

Blue light-emitting polymers, such as PF, are of keen interest since they can be utilized either as a blue light source or as the host material for generation of other colors *via* energy transfer to fluorophores of lower energy [14]. However, one of the major troubles in obtaining blue EL from PFs is the long-range emission (green region). It is attributed to aggregation [15–17], originating from inter-chain attractions in the π-conjugated systems, or excimer formation by keto defects [18–20], inducing an energy transfer of singlet excitons. Since the distance between the polymer chains is expected to be a crucial governing factor for the formation of aggregates [21,22], several researchers have attempted to restrain the green emission by introducing a bulky end group [23] or crosslinkable group [24–26]. In conjugated polymers, the molecular architecture strongly influences the microcrystalline organization, to generate the change of the optoelectronic properties [27]. Spiro-shaped molecules based on 9,9′-spirobifluorene [28–30], prepared by connecting two identically substituted-fluorene moieties to form an sp^3-hybridized carbon atom, have been introduced as EL materials. The spiro-shaped PFs with two separate π-systems connected by a spiro linkage showed interactions between the aromatic spiro segment and backbone of other polymers [31]. And, the alkoxy groups in the spiro-fluorene moiety could achieve a better solubility and processability of aromatic conjugated polymers [26].

In our previous contribution, synthesis and properties of a new EL polymer utilizing a new backbone, poly(2,6-(4,4-bis-(2-ethylhexyl)-4*H*-cyclopenta[*def*]phenanthrene)) (PCPP), with stabilized pure blue emission has been reported. EL spectrum of PCPP did not show any peak between 500 and 600 nm, which would correspond to keto

---

* Corresponding author. Tel.: +82 51 510 2203; fax: +82 51 516 7421.
E-mail address: hssuh@pusan.ac.kr (H. Suh).

0032-3861/$ – see front matter Crown Copyright © 2008 Published by Elsevier Ltd. All rights reserved.
doi:10.1016/j.polymer.2008.10.012

defect sites or aggregates/excimers, even after annealing the device at 150 °C or operation of the device in air [5,6]. Herein, we report the synthesis and properties of a new EL polymer, utilizing a new backbone, poly(2,6-(3′,6′-bis(2-ethylhexyloxy)-4,4′-spirobi(4*H*-cyclopenta[*def*]phenanthrene))) (spiro-PCPP), with a spiro-structure and cyclopentaphenanthrene backbone.

2. Experimental section

2.1. Instrumental characterization

All reagents were purchased from Aldrich or TCI and used without further purification. Solvents were purified by normal procedure and handled under moisture-free atmosphere. ^{1}H and ^{13}C NMR spectra were recorded with a Varian Gemini-300 (300 MHz) spectrometer and chemical shifts were recorded in ppm units with TMS as the internal standard. Flash column chromatography was performed with Merck silica gel 60 (particle size 230–400 mesh ASTM) with ethyl acetate/hexane or methanol/methylene chloride gradients unless otherwise indicated. Analytical thin layer chromatography (TLC) was conducted using Merck 0.25 mm silica gel 60F precoated aluminum plates with fluorescent indicator UV254. High resolution mass spectra (HRMS) were recorded on a JEOL JMS-700 mass spectrometer under electron impact (EI) or fast atom bombardment (FAB) conditions in the Korea Basic Science Institute (Daegu, Korea). Melting points were determined on an Electrothermal model IA 9100 micro-melting point apparatus. Molecular weight and polydispersity of the polymer were determined by gel permeation chromatography (GPC) analysis with a polystyrene standard calibration. Differential scanning calorimetry (DSC) analysis was performed under a nitrogen atmosphere (50 mL/min) on a DSC 822 at heating rates of 10 °C/min. Thermogravimetric analysis (TGA) was performed with a Dupont 951 TGA instrument in a nitrogen atmosphere at a heating rate of 10 °C/min to 800 °C. The UV–vis absorption spectra were recorded by a Varian Cary 1 spectrophotometer, while the Oriel InstaSpec IV CCD detection system with arc-xenon lamp was used for the photoluminescence and electroluminescence spectra measurements.

2.2. EL device fabrication and measurements

For the EL experiment, poly(3,4-ethylenedioxythiophene) (PEDOT) doped with poly(styrenesulfonate) (PSS), as the hole-injection-transport layer, was introduced between emissive layer and ITO glass substrate cleaned by successive ultrasonic treatments. The solution of the PEDOT:PSS in aqueous isopropyl alcohol was spin-coated on the surface-treated ITO substrate and dried on a hot plate for 30 min at 110 °C. On top of the PEDOT layer, the emissive polymer film was obtained by spin casting chlorobenzene solution of the polymer. The emissive polymer thin film prepared had a uniform surface with a thickness of around 110 nm. The emissive film was dried in vacuum, and calcium (20 nm) and aluminum (100 nm) electrodes were deposited on the top of the polymer films through a mask by vacuum evaporation at pressures below 10^{-7} Torr, yielding active areas of 4 mm^{2}. For the determination of device characteristics, current density–voltage (*J*–*V*) and luminance–voltage (*L*–*V*) characteristics of the devices were measured using a Keithley 2400 Source Measure Unit equipped with a calibrated photo-multiplier tube.

2.3. Synthesis of monomer and polymer

2.3.1. 8,9-Dihydro-4H-cyclopenta[def]phenanthrene (**2**)

The mixture of 4*H*-cyclopenta[*def*]phenanthrene (**1**) (1.45 g, 7.62 mmol), 10% palladium–charcoal (300 mg), and methanol/dichloromethane (40 mL/40 mL) was shaken for 15 h at room temperature under a hydrogen atmosphere (60 psi). After removal of the catalyst by filtration, the solvent was evaporated under reduced pressure. The residue was purified by flash column chromatography to give 1.46 g (99.6%) of compound **2** as white solid: mp 134 °C; R_f 0.44 (SiO_2, 100% hexane). ^{1}H NMR (300 MHz, $CDCl_3$): *δ* (ppm) 3.18 (s, 4H), 3.92 (s, 2H), 7.17 (d, 2H, *J* = 7.4 Hz), 7.24 (t, 2H, *J* = 7.4 Hz), 7.37 (d, 2H, *J* = 7.4 Hz); ^{13}C NMR (75 MHz, $CDCl_3$): *δ* (ppm) 26.51, 37.69, 122.95, 124.92, 127.51, 130.76, 139.65, 140.67. HRMS (*m*/*z*, EI^{+}) calcd for $C_{15}H_{12}$ 192.0939, found 192.0943.

2.3.2. 2,6-Dibromo-8,9-dihydro-4H-cyclopenta[def]phenanthrene (**3**)

To prepare copper bromide adsorbed on alumina, a solution of 10 g of copper bromide in 30 mL of distilled water was treated with neutral alumina (20 g, Merck aluminum oxide 90 active neutral) at room temperature. The reaction mixture was concentrated at 80 °C under reduced pressure. The resulting residue was dried under vacuum (4 Torr) at 100 °C for 15 h to generate copper bromide adsorbed on alumina. To a stirred solution of 1.87 g (3.59 mmol) of 8,9-dihydro-4*H*-cyclopenta[*def*]phenanthrene (**2**) in 70 mL of carbon tetrachloride at room temperature was added 31.6 g of copper bromide adsorbed on alumina. After 5 h at 60 °C, the solid was filtered and washed with 2 × 30 mL of carbon tetrachloride. The combined organic phase was concentrated under reduced pressure and purified by flash column chromatography to give 3.36 g (99%) of compound **3** as pale yellow solid: mp 184 °C; R_f 0.50 (SiO_2, 100% hexane). ^{1}H NMR (300 MHz, $CDCl_3$): *δ* (ppm) 3.08 (s, 4H), 3.83 (s, 2H), 7.46 (s, 2H), 7.47 (s, 2H); ^{13}C NMR (75 MHz, $CDCl_3$): *δ* (ppm) 25.95, 37.35, 121.33, 126.43, 128.43, 131.91, 137.56, 141.81. HRMS (*m*/*z*, EI^{+}) calcd for $C_{15}H_{10}Br_2$ 347.9149, found 347.9153.

2.3.3. 2,6-Dibromo-4H-cyclopenta[def]phenanthrene (**4**)

To a stirred solution of 3.15 g (9.05 mmol) of 2,6-dibromo-8,9-dihydro-4*H*-cyclopenta[*def*]phenanthrene (**3**) in 70 mL of carbon disulfide at room temperature was added dropwise 0.56 mL (10.85 mmol) of Br_2 in carbon disulfide over 3 h. The reaction mixture was stirred for 1 h, concentrated under reduced pressure, and purified by flash column chromatography to give 3.15 g (100%) of compound **4** as pale yellow solid: mp 210 °C; R_f 0.53 (SiO_2, 100% hexane). ^{1}H NMR (300 MHz, $CDCl_3$): *δ* (ppm) 4.32 (s, 2H), 7.75 (s, 2H), 7.80 (s, 2H), 7.99 (s, 2H); ^{13}C NMR (75 MHz, $CDCl_3$): *δ* (ppm) 37.16, 125.31, 125.62, 126.41, 127.97, 128.97, 132.91, 143.03. HRMS (*m*/*z*, EI^{+}) calcd for $C_{15}H_8Br_2$ 345.8993, found 345.8993.

2.3.4. 2,6-Dibromo-4H-cyclopenta[def]phenanthren-4-one (**5**)

A solution of 2,6-dibromo-4*H*-cyclopenta[*def*]phenanthrene (**4**) (1 g, 2.87 mmol) in benzene (60 mL) was stirred with activated MnO_2 (10 g). After 1 h at 60 °C, the solid was filtered and washed with 3 × 30 mL of benzene. The combined organic phase was concentrated under reduced pressure and purified by flash column chromatography to give 560 mg (53.7%) of compound **5** as yellow powder: mp 166–167 °C; R_f 0.32 (SiO_2, methylene chloride:hexane = 1:10). ^{1}H NMR (300 MHz, $CDCl_3$): *δ* (ppm) 7.72 (s, 2H), 7.90 (d, 2H, *J* = 1.1 Hz), 8.09 (d, 2H, *J* = 1.3 Hz); ^{13}C NMR (75 MHz, benzene-d_6): *δ* (ppm) 124.27, 126.72, 126.79, 129.52, 133.97, 135.14, 137.89, 190.08. HRMS (*m*/*z*, EI^{+}) calcd for $C_{15}H_6Br_2O$ 359.8785, found 359.8781.

2.3.5. 2-Bromo-5,3′-dimethoxybiphenyl (**7**)

3,3′-Dimethoxybiphenyl (**6**) (5.0 g, 23.34 mmol) was dissolved in dimethylformamide. *N*-Bromosuccinimide (4.15 g, 23.34 mmol) was dissolved in dimethylformamide (63 mL) and added slowly to a solution of 3,3′-dimethoxybiphenyl for about 1.5 h. The mixture was stirred at room temperature for about 12 h and distilled water was added thereto, followed by stirring for about 10 min. The combined organic phase was concentrated under reduced pressure and purified by flash column chromatography to give 6.7 g (98%) of compound **7** as colorless oil: R_f 0.30 (SiO_2, ethyl acetate:hexane = 1:50). ^1H NMR (300 MHz, $CDCl_3$): δ (ppm) 3.83 (s, 3H), 3.87 (s, 3H), 6.81 (dd, 1H, *J* = 8.8 Hz and 3.1 Hz), 6.92 (d, 1H, *J* = 3.1 Hz), 7.03–6.95 (m, 3H), 7.37 (t, 1H, *J* = 7.7 Hz), 7.56 (d, 1H, *J* = 8.8 Hz); ^{13}C NMR (75 MHz, $CDCl_3$) δ (ppm) 55.7, 55.9, 113.4, 113.7, 115.2, 115.4, 117.0, 122.1, 129.4, 134.1, 142.9, 143.7, 159.2, 159.5. HRMS (*m*/*z*, EI^+) calcd for $C_{14}H_{13}Br_1O_2$ 292.0099, found 292.0103.

2.3.6. 6-Bromo-biphenyl-3,3′-diol (*8*)

A solution of boron tribromide (17.9 mL, 17.9 mmol) was slowly added to a solution of 2-bromo-5,3′-dimethoxybiphenyl (**7**) (2.5 g, 8.5 mmol) at 0 °C, followed by stirring for 1 h. Purification by silica gel chromatography using 4% ethyl acetate in dichloromethane gave 1.78 g (79%) of compound **8** as white solid: mp 111 °C; R_f 0.30 (SiO_2, ethyl acetate:hexane = 1:50). ^1H NMR (300 MHz, $CDCl_3$) δ (ppm) 5.54 (s, 1H), 5.73 (s, 1H), 6.92–6.68 (m, 5H), 7.25 (m, 1H), 7.44 (d, 1H); ^{13}C NMR (75 MHz, $CDCl_3$) δ 112.8, 114.7, 116.2, 116.3, 118.1, 121.8, 129.2, 133.9, 142.3, 143.1, 154.9, 155.0. HRMS (*m*/*z*, EI^+) calcd for $C_{12}H_9Br_1O_2$ 263.9786, found 263.9781.

2.3.7. 2-Bromo-3′,5-bis[(2-ethylhexyl)oxy]-1,1′-biphenyl (*9*)

The obtained 6-bromo[1,1′-biphenyl]-3,3′-diol (**8**) (3.9 g, 14.9 mmol), ethylhexyl bromide (6.6 mL, 37.25 mmol), potassium carbonate (12.4 g, 89.4 mmol) and potassium iodide (2.5 g, 14.9 mmol) were dissolved in dimethylformamide (150 mL), followed by heating for about 24 h at about 150 °C. After the reaction mixture was cooled to room temperature, water and hexane were added. The aqueous phase was extracted with hexane and combined organic layers were dried over $MgSO_4$. The solvent was removed under vacuum and the residue was purified by column chromatography to give 6.2 g (85.2%) of compound **9** as colorless oil: R_f 0.15 (SiO_2, methylene chloride:hexane = 1:20). ^1H NMR (300 MHz, $CDCl_3$): δ (ppm) 0.92–1.00 (m, 12H), 1.35–1.58 (m, 16H), 1.71–1.80 (m, 2H), 3.86 (d, 2H, *J* = 5.8 Hz), 3.91 (d, 2H, *J* = 5.8 Hz), 6.78–6.87 (m, 2H), 6.93 (d, 1H, *J* = 3.0 Hz), 6.94–7.02 (m, 2H), 7.34 (t, 1H, *J* = 7.4 Hz), 7.54 (d, 1H, *J* = 8.8 Hz); ^{13}C NMR (75 MHz, $CDCl_3$): δ (ppm) 11.09, 14.05, 23.01, 29.05, 30.50, 39.37, 70.60, 112.61, 113.90, 115.28, 115.56, 117.23, 121.44, 128.84, 133.56, 142.45, 143.28, 158.57, 158.96. HRMS (*m*/*z*, EI^+) calcd for $C_{28}H_{41}BrO_2$ 488.2290, found 488.2291.

2.3.8. 2,6-Dibromo-(3′,6′-bis(2-ethylhexyloxy)-spiro(4H-cyclopenta[def]phenanthrene-4,9′-[9H]fluorene)) (*10*)

2-Bromo-3′,5-bis[(2-ethylhexyl)oxy]-1,1′-biphenyl (**9**) (5.67 g, 11.6 mmol) was dissolved in dried THF (30 mL) and cooled to −78 °C. Then, 1.7 M *t*-butyllithium (14.67 mL, 24.94 mmol) was added slowly. The obtained resultant was stirred for 1 h at −78 °C. After 1 h, 2,6-dibromo-4*H*-cyclopenta[*def*]phenanthren-4-one (**5**) (2.1 g, 5.8 mmol) dissolved in dried THF (30 mL) was added slowly, stirred for about 1 h, allowed to warm to room temperature and further stirred at room temperature for about 30 min. The aqueous phase was extracted with hexane and the solvent was removed under vacuum and the residue was mixed with acetic acid (50 mL) and hydrochloric acid (1 mL) and stirred for about 22 h at room

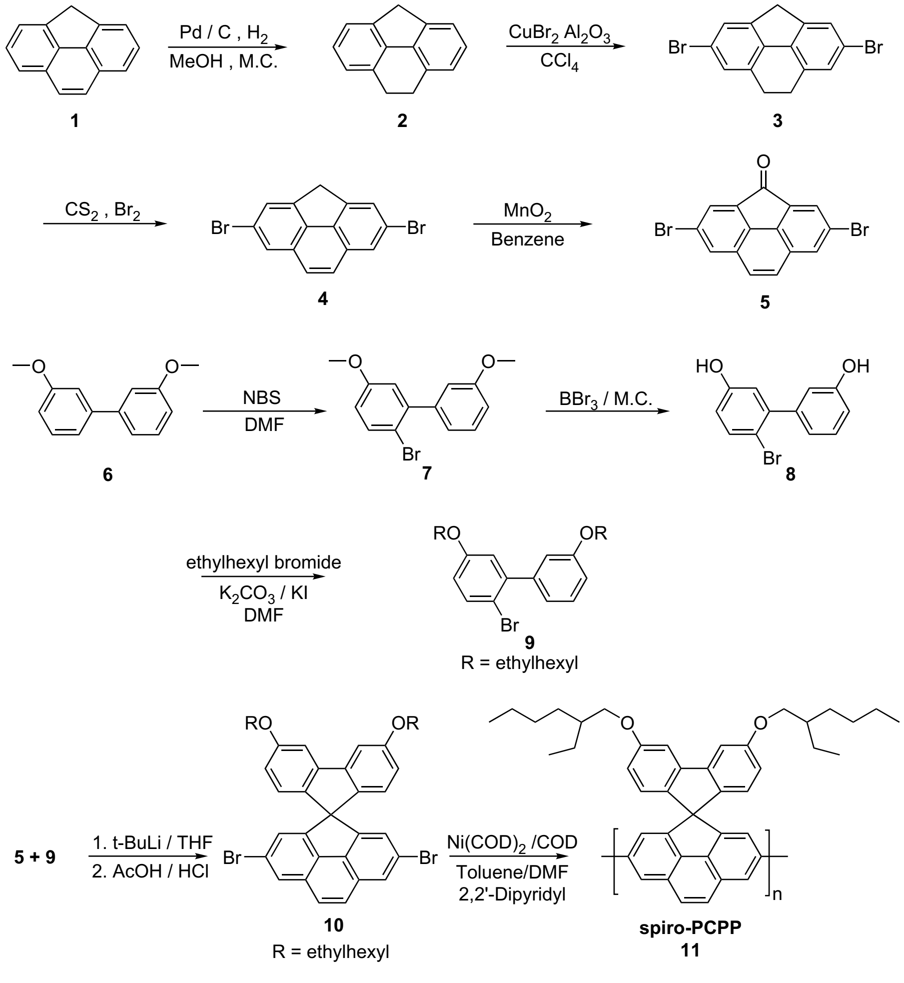

Scheme 1. Synthetic routes for the monomer and the spiro-PCPP.

Table 1
Characterization of the polymer.

Polymer	Yield (%)	M_n[a]	M_w[a]	PDI[a]	T_g[b] (°C)	T_d[c] (°C)
Spiro-PCPP	46	71,000	225,000	3.2	85	417

[a] Molecular weight (M_w) and polydispersity (PDI) of the polymer were determined by gel permeation chromatography (GPC) in THF using polystyrene standards.
[b] Glass transition temperature measured by DSC under N_2.
[c] Onset decomposition temperature (5% weight loss) measured by TGA under N_2.

temperature. The reaction mixture was concentrated under reduced pressure, and purified by flash column chromatography to give 1.83 g (41.9%) of compound **10** as white powder: mp 121 °C; R_f 0.15 (SiO_2, methylene chloride:hexane = 2:5). ^1H NMR (300 MHz, $CDCl_3$): δ (ppm) 0.92–1.01 (m, 12H), 1.35–1.57 (m, 16H), 1.72–1.82 (m, 2H), 3.95 (d, 4H, $J = 5.8$ Hz), 6.48 (d, 2H, $J = 8.5$ Hz), 6.66 (d of d, 2H, $J = 2.2$ and 8.4 Hz), 7.13 (d, 2H, $J = 1.4$ Hz), 7.41 (d, 2H, $J = 2.2$ Hz), 7.85 (s, 2H), 7.99 (d, 2H, $J = 1.1$ Hz); ^{13}C NMR (75 MHz, $CDCl_3$): δ (ppm) 11.19, 14.09, 23.06, 23.96, 29.14, 30.60, 39.53, 66.40, 70.69, 106.07, 114.62, 122.47, 123.95, 124.66, 125.56, 126.35, 128.71, 135.79, 138.47, 143.10, 149.83, 160.16. HRMS (m/z, FAB^+) calcd for $C_{43}H_{47}Br_2O_2$ 753.1943, found 753.1943.

*2.3.9. Poly(2,6-(3′,6′-bis(2-ethylhexyloxy)-spiro(4H-cyclopenta[def]phenanthrene-4,9′-[9H]fluorene))) (spiro-PCPP) (**11**)*

In a three-necked flask were placed bis(1,5-cyclooctadiene)-nickel(0) ($Ni(COD)_2$) (481 mg, 1.75 mmol), 2,2-dipyridyl (276 mg, 1.75 mmol), cyclooctadiene (214 mL, 1.75 mmol), and DMF (8 mL). After three freezing–thaw cycles, the catalyst was heated to 80 °C for 30 min to form the purple complex. The reaction mixture was treated with 600 mg (0.80 mmol) of 2,6-dibromo-3′,6′-bis(2-ethylhexyloxy)-4,4′-spirobi(4*H*-cyclopenta[*def*]phenanthrene) (**10**) in 8 mL of toluene, and heated at 80 °C for 4 days. After cooling to room temperature, the reaction mixture was poured into the mixture of 100 mL of 1 N HCl solution, 100 mL of acetone, and 200 mL of methanol, and stirred for 6 h. The precipitate was filtered, redissolved in chloroform and precipitated again with large amount methanol. The obtained pale yellow solid was dried in vacuum at 60 °C for 48 h to give 218 mg (46%) of spiro-PCPP (**11**) as a yellowish white solid. ^1H NMR (300 MHz, THF-d_4): δ (ppm) 0.92–0.97 (m, 12H), 1.36–1.49 (m, 18H), 3.98 (m, 4H), 6.40–6.43 (m, 2H), 6.53–6.55 (m, 2H), 7.16 (s, 2H), 7.44 (s, 2H), 7.90 (s, 2H), 8.00 (s, 2H).

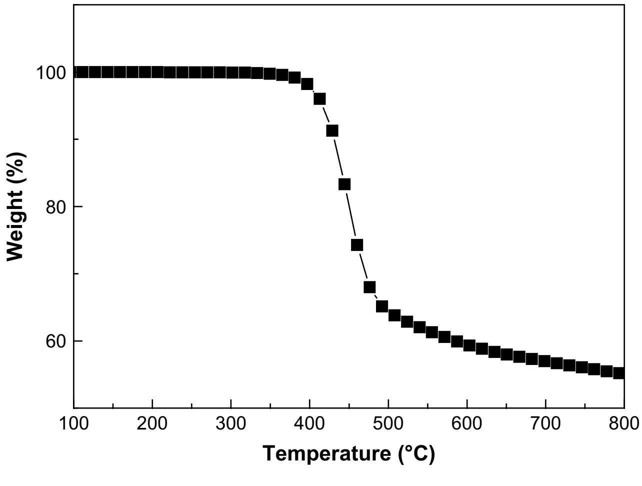

Fig. 1. Thermogravimetric analysis of the polymer under N_2.

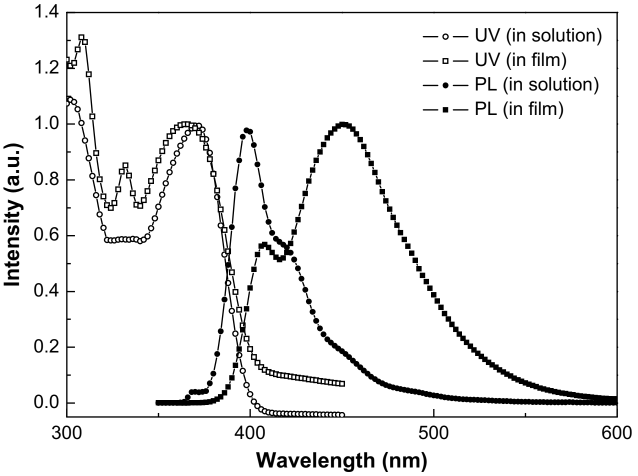

Fig. 2. UV–vis absorption and photoluminescence spectra of polymer in the THF solution and film.

3. Results and discussion

3.1. Synthesis and characterization

The general synthetic routes toward the monomer and polymer are outlined in Scheme 1. In the first step, 4*H*-cyclopenta[*def*]phenanthrene (**1**) was hydrogenated using Pd/C to generate 8,9-dihydro-4*H*-cyclopenta[*def*]phenanthrene (**2**). Alumina-supported copper(II) bromide [32] was used for the bromination to provide 2,6-dibromo-8,9-dihydro-4*H*-cyclopenta[*def*]phenanthrene (**3**). Subsequent dehydrogenation [33] using bromine and carbon disulfide provided 2,6-dibromo-4*H*-cyclopenta[*def*]phenanthrene (**4**). Oxidation of compound **4** by MnO_2 corresponding 2,6-dibromo-4*H*-cyclopenta[*def*]phenanthren-4-one (**5**) occurred in good yield. 2-Bromo-5,3′-dimethoxybiphenyl (**7**) was prepared from monobromination of 3,3′-dimethoxybiphenyl (**6**). Demethylation of compound **7** gave 6-bromo-biphenyl-3,3′-diol (**8**), and alkylation with 1-octyl bromide gave 2-bromo-3′,5-bis[(2-ethylhexyl)oxy]-1,1′-biphenyl (**9**). Compound **9** was treated with *t*-BuLi and 2,6-dibromo-4*H*-cyclopenta[*def*]phenanthren-4-one to generate a tertiary alcohol, which was cyclized to give 2,6-dibromo-3′,6′-bis(2-ethylhexyloxy)-4,4′-spirobi(4*H*-cyclopenta[*def*]phenanthrene) (**10**) and its geometric isomer [21]. Separation of geometrical isomers between major compound can be achieved from column chromatography from a mixed solvent of *n*-hexane and dichloromethane. Polymerization of the monomer **10** was affected under Yamamoto condition [34], using bis(1,5-cycloocta-diene)nickel(0) catalyst, 2,2′-dipyridyl, and cyclooctadiene.

The resulting polymer was soluble in common organic solvents such as chloroform, chlorobenzene, tetrahydrofuran (THF), dichloromethane and *o*-dichlorobenzene (ODCB). Table 1 summarizes the polymerization results including molecular weights, PDI and thermal stability of the polymer. The number-average (M_n) and weight-average molecular weight (M_w) of the spiro-PCPP were 71,000 and 225,000, respectively, with polydispersity index (PDI,

Table 2
Characteristics of the UV–vis absorption, photoluminescence, and electroluminescence spectra.

Conditions	Abs λ_{max} (nm)	PL λ_{max}[a] (nm)	Fwhm[b] of PL	QE_{PL} (%)
Solution	371	398	37	85
Film	364	451 (406)	89	–

[a] The data in the parentheses are the wavelengths of shoulders and subpeaks.
[b] Full width at half-maximum of PL and EL spectra.

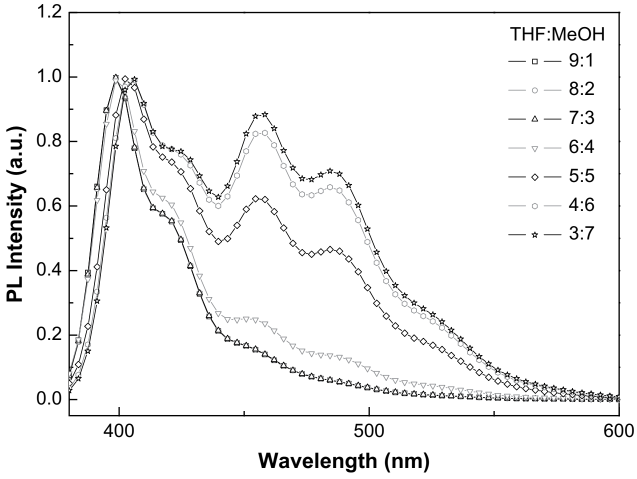

Fig. 3. Photoluminescence spectra of spiro-PCPP ([spiro-PCPP] = 1×10^{-5} M) in mixture with changing ratio of THF and MeOH (THF:MeOH = 9:1–3:7). All emission scans were collected by exciting at 350 nm.

M_w/M_n) of 3.2. The thermal properties of the polymer were evaluated by DSC and TGA under nitrogen atmosphere. The polymer showed good thermal stability with a glass transition temperature (T_g) of 85 °C, using DSC performed at a temperature range of 30–250 °C. As shown in Fig. 1, decomposition temperature (T_d) is 417 °C for spiro-PCPP, exhibiting good thermal stability, an important quality for application in flat panel displays.

3.2. Photophysical properties

Table 3
Electrochemical potentials and energy levels of the polymer.

Polymer	Optical bandgap[a] (eV)	Chemical bandgap[b] (eV)	E_{ox}[c] (V)	E_{red}[c] (V)	HOMO[d] (eV)	LUMO[e] (eV)
Spiro-PCPP	3.00	2.35	1.10	−1.25	−5.90	−2.90

[a] Optical energy bandgap was estimated from the onset wavelength of the optical absorption.
[b] Calculated from the E_{ox} and E_{red}.
[c] Onset oxidation and reduction potential measured by cyclic voltammetry.
[d] Calculated from the oxidation potentials.
[e] Calculated from the HOMO energy levels and E_g.

The UV–vis absorption and photoluminescence (PL) emission spectra of the polymer as solution and a thin film are shown in Fig. 2. The solution was prepared using THF as a solvent and the thin film by spin-coating on quartz plates from the polymer solution in chlorobenzene. The absorption and emission data for the polymer are summarized in Table 2. There is little difference between the absorption spectra of the solution and the thin film of the polymer, which can be attributed to the π–π* transitions of the polymer. The maximum absorption peak appeared at 371 nm in chloroform. By comparing the UV–vis spectra of the spiro-monomer **10**, PCPP monomer and spiro-PCPP polymer [5], it was found that the peak at 335 nm is originating from the aromatic spiro-portion. The maximum absorption peak of the polymer film appeared at 364 nm, which was blue-shifted about 7 nm. This PL spectrum displays a vibronic fine structure with emission band at 415 nm. The PL spectra of the polymer were measured by the excitation of 350 nm. The PL emission spectrum of the polymer in the THF solution shows a maximum peak at 398 nm, nearly identical with that of PCPP [25]. The PL spectrum of the solid thin film displayed maximum peak appearing at 451 nm, which is red-shifted over 50 nm from that of the solution, caused by the inter-chain interaction of the polymers. In the solid thin film, the blue emission at 406 nm for the π–π* transition of the conjugated polymer backbone is decreased, and the maximum peak appeared at around 451 nm.

As shown in Fig. 3, the PL spectra of spiro-PCPP ([spiro-PCPP] = 1×10^{-5} M) in mixture with changing ratio of THF and MeOH (THF:MeOH = 9:1–3:7) were collected by exciting at 350 nm. The PL spectra of the spiro-PCPP with 9:1–7:3 ratios of THF and MeOH were not changing with the maximum peak at 398 nm. With 6:4–3:7 ratios of THF and MeOH, the maximum peak at 398 nm was shifted to 406 nm. With an increased ratio of the hydrophilic solvent (MeOH), the inter-chain interaction of the hydrophobic polymers was enhanced to show the peaks at 458 and 484 nm. This phenomenon can be also explained by the increased inter-chain interaction as happening in the solid thin film state. The PL maximum peak of the spiro-PCPP with solid thin film appeared at 451 nm, unlike the long wavelength emission of PF with maximum peak at 550 nm. Quantum yield (Φ_{PL}) in solution was determined in chloroform, relative to 9,10-diphenylanthracene as the standard ($\Phi_{PL} = 0.91$ in ethanol) [35]. Spiro-PCPP has a maximal efficiency of 85%.

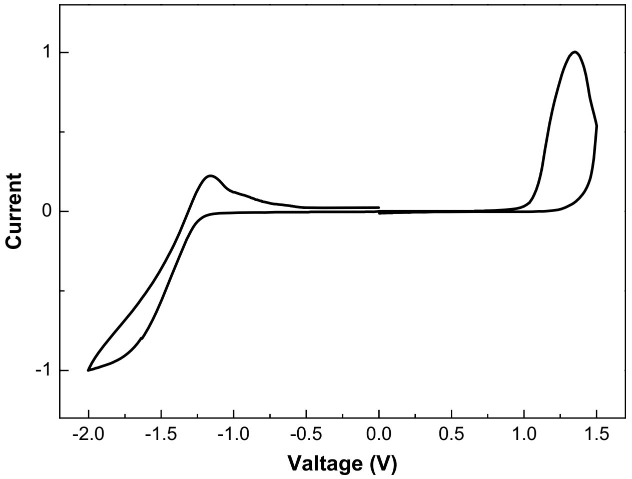

Fig. 4. Cyclic voltammetry curve of the polymer in 0.1 M Bu_4NBF_4 acetonitrile solution at a scan rate of 100 mV/s at room temperature (vs an Ag quasi-reference electrode).

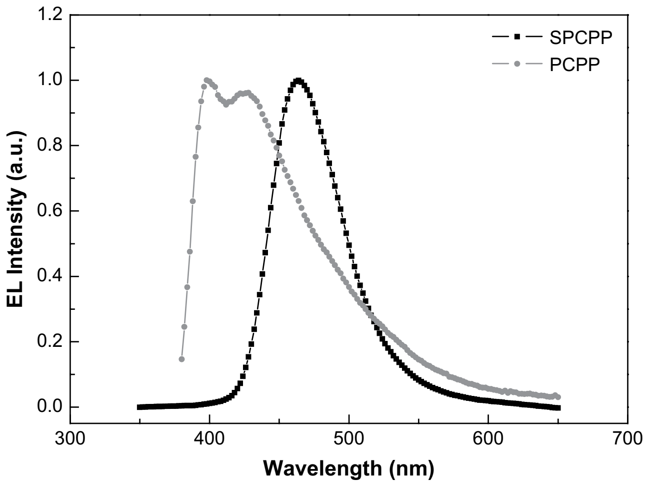

Fig. 5. Electroluminescence spectra of devices with the configuration of ITO/PEDOT/polymers/Ca:Al.

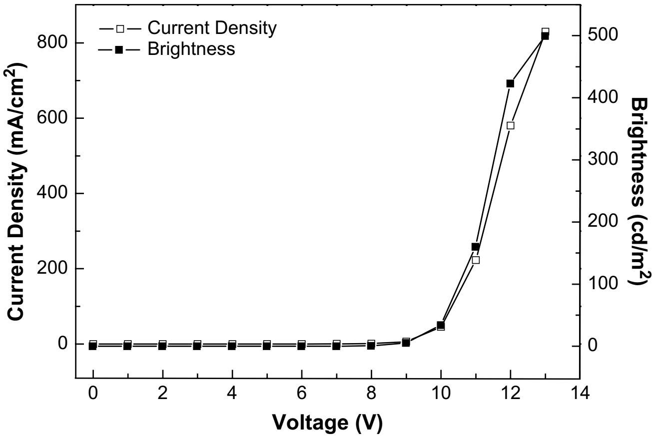

Fig. 6. Current–voltage–luminescence (*I*–*V*–*L*) characteristics of OLED with the configuration of ITO/PEDOT/polymer/Ca:Al.

3.3. Electrochemical properties of the polymer

The electrochemical properties of the polymer were determined from the bandgap estimated from the absorption onset wavelength, and the HOMO energy level which was estimated from the cyclic voltammetry (CV). The CV was performed with a solution of tetrabutylammonium tetrafluoroborate (Bu_4NBF_4) (0.10 M) in acetonitrile at a scan rate of 100 mV/s at room temperature under the protection of argon. A platinum electrode (~0.05 cm^2) coated with a thin polymer film was used as the working electrode. Pt wire and $Ag/AgNO_3$ electrode were used as the counter electrode and reference electrode, respectively. The energy level of the $Ag/AgNO_3$ reference electrode (calibrated by the Fc/Fc^+ redox system) was 4.8 eV below the vacuum level. The CV spectrum is shown in Fig. 4, and the oxidation potential derived from the onset of electrochemical p-doping is summarized in Table 3. HOMO level was calculated according to the empirical formula $E_{HOMO} = -([E_{onset}]^{ox} + 4.8)$ (eV). During the anodic scan, the oxidation onset potential of the polymer is 1.10 V, and exhibited irreversible p-doping process. HOMO energy level of the polymer was approximately −5.90 eV. The onset potential of reduction for spiro-PCPP is located at −1.25 eV. The electrochemical bandgap, calculated from cyclic voltammetry data, is about 2.35 eV, somewhat lower than the optical bandgap estimated from the onset absorption of the polymer solution. The optical bandgap was estimated from absorption onset of the polymer. The LUMO energy level was calculated from the values of the bandgap and HOMO energy level. The value of the LUMO energy level of the polymer is −2.90 eV.

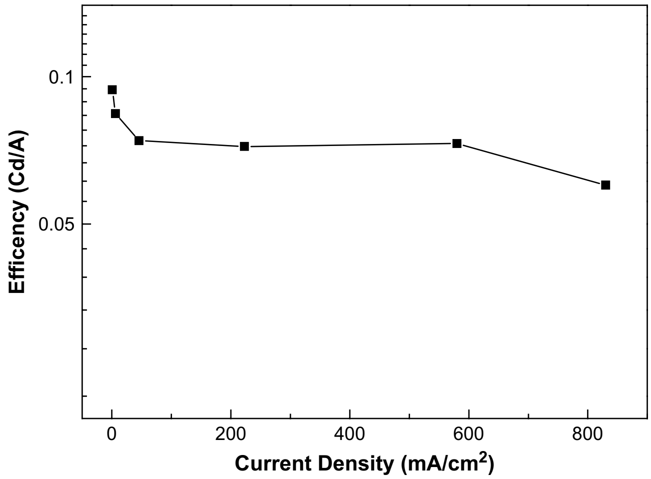

Fig. 7. Efficiency of OLEDs of polymer with the configuration of ITO/PEDOT/spiro-PCPP/Ca:Al.

Table 4
Device performance characteristics of polymer.

Polymer	Turn-on voltage[a] (V)	Voltage[b] (V)	Current density[b] (mA/cm^2)	Luminance[b] (cd/m^2)	LE_{max}[c] (cd/A)	CIE (x, y)[d]
Spiro-PCPP	8	13	830	500	0.10	(0.15, 0.08)

[a] Voltages required to achieve a brightness of 1 cd/m^2.
[b] Measured under the condition of maximum brightness.
[c] Maximum luminescence efficiency.
[d] Calculated from the EL spectrum.

3.4. Electroluminescent properties

The electroluminescence (EL) performance of the polymer was examined in the device configuration of ITO/PEDOT:PSS/polymer/Ca:Al. The typical EL spectrum from such device is shown in Fig. 5. The EL spectrum of spiro-PCPP shows maximum peaks at 463 nm. The maximum peak of the spectrum of spiro-PCPP is red-shifted by 63 nm as compared to the case of PCPP. This phenomenon is caused by inter-chain interaction of the polymers. The device of spiro-PCPP with the configuration of ITO/PEDOT/polymer/Ca:Al showed the emission color of sky blue with CIE coordinates of (0.14, 0.15). The current density–voltage (*J*–*V*) and luminescence–voltage (*V*–*L*) characteristics of ITO/PEDOT/polymer/Ca:Al device are shown in Fig. 6. The turn-on voltage of device was about 8 V. The luminescence intensity of the polymer increased with an increase in voltage, and the maximum luminescence (L_{max}) of spiro-PCPP device is 500 cd/m^2 at 13 V. As shown in Fig. 7, the maximum luminescence efficiency of spiro-PCPP at room temperature is 0.10 cd/A. Spiro-PCPP has been reported as new conjugated backbones with high efficiencies. Introduction of spiro group in PCPPs can change the device performance to result in red-shifted spectra of PL and EL and reduction of the luminescence efficiency of the device since spiro group and cyclopenta[*def*]phenanthrene backbone induce inter-chain interaction (Table 4).

4. Conclusion

We present here the synthesis of a new conjugated polymer, spiro-PCPP. The polymer was synthesized by the Yamamoto polymerization. The PL emission spectrum in THF solution showed maximum peak at 398 nm, nearly identical with that of PCPP. PL spectrum of solid state exhibited maximum peak at 451 nm, which was red-shifted over 50 nm from that of the solution, caused by the inter-chain interaction of the polymers. The PL spectra of spiro-PCPP in THF:MeOH from 9:1 to 3:7 showed increasing peaks at 458 and 484 nm, also caused by the same inter-chain interaction of the polymers. This phenomenon has the same tendency as compared to the PL spectrum in solid thin film state with increased inter-chain interaction. Therefore, we can conclude that the inter-chain interaction between aromatic spiro group and the backbone of PCPP induce the red-shifted color emission. The polymer LED with the configuration of ITO/PEDOT/polymer/Ca:Al showed the emission color of sky blue with CIE coordinates of (0.14, 0.15), which are close to those of the standard blue (0.14, 0.08). The maximum luminescence (L_{max}) of the LED with spiro-PCPP was 500 cd/m^2 at 13 V.

Acknowledgment

This work was supported for two years (2007–2009) by Pusan National University Research Grant (H. Suh).

References

[1] Gustafsson G, Cao Y, Treacy GM, Klavetter F, Colaneri N, Heeger AJ. Nature 1992;357:477.
[2] Jin Y, Jee J, Kim K, Kim J, Song S, Park SH, et al. Polymer 2007;48:1541.
[3] Guo TF, Pyo S, Chang SC, Yang Y. Adv Funct Mater 2001;11:339.
[4] Wen GA, Xin Y, Zhu XR, Zeng WJ, Zhu R, Feng JC, et al. Polymer 2007;48:1824.
[5] Suh H, Jin Y, Park SH, Kim D, Kim J, Kim C, et al. Macromolecules 2005;38:6285.
[6] Park SH, Jin Y, Kim JY, Kim SH, Kim J, Suh H, et al. Adv Funct Mater 2007;17:3063.
[7] Yang C, Scheiber H, List EJW, Jacob J, Mullen K. Macromolecules 2006;39:5213.
[8] Grisorio R, Suranna GP, Mastrorilli P, Nobile CF. Org Lett 2007;9:3149.
[9] Grell M, Bradley DDC, Inbasekaran M, Woo EP. Adv Mater 1997;9:798.
[10] Jin Y, Kim JY, Song S, Xia Y, Kim J, Woo HY, et al. Polymer 2008;49:467.
[11] Zhao W, Cao T, White JM. Adv Funct Mater 2004;14:783.
[12] Jin Y, Ju J, Kim J, Lee S, Kim JY, Park SH, et al. Macromolecules 2003;36:6970.
[13] Greenham NC, Morattl SC, Bradley DDC, Friend RH, Holmes AB. Nature 1993;365:628.
[14] McGehee MD, Bergstedt T, Zhang C, Saab AP, O'Regan MB, Bazan GC, et al. Adv Mater 1999;11:1349.
[15] Montilla F, Mallavia R. Adv Funct Mater 2007;17:71.
[16] Harre K, Wegner G. Polymer 2006;47:7312.
[17] Bliznyuk VN, Carter SA, Scott JC, Klärner G, Miller RD, Miller DC. Macromolecules 1999;32:361.
[18] Scherf U, List EJW. Adv Mater 2002;14:477.
[19] Yang CH, Bhongale CJ, Chou CH, Yang SH, Lo CN, Chen TM, et al. Polymer 2007;48:116.
[20] Gong X, Iyer PK, Moses D, Bazan GC, Heeger AJ. Adv Funct Mater 2003;13:325.
[21] Nguyen TC, Martini IB, Lie J, Schwartz BJ. J Phys Chem B 2000;104:237.
[22] Shi Y, Liu J, Yang Y. J Appl Phys 2000;87:4254.
[23] Klärner G, Miller RD, Hawker C. J Polym Prepr 1998;39:1006.
[24] Wu G, Yang C, Fan B, Zhang B, Chen X, Li Y. J Appl Polym Sci 2006;100:2336.
[25] Klärner G, Lee JI, Lee VY, Chan E, Chen JP, Nelson A, et al. Chem Mater 1999;11:1800.
[26] Lee H, Oh J, Chu HY, Lee JI, Kim SH, Yang YS, et al. Tetrahedron 2003;59:2773.
[27] Surin M, Hennebicq E, Ego C, Marsitzky D, Grimsdale AC, Mullen K, et al. Chem Mater 2004;16:994.
[28] Marsitzky D, Murray J, Scott JC, Carter KR. Chem Mater 2001;13:4285.
[29] Reddy DS, Chou CH, Shu CF, Lee GH. Polymer 2003;44:557.
[30] Yu WL, Pei J, Huang W, Heeger AJ. Adv Mater 2000;12:828.
[31] King SM, Hintschich SI, Dai D, Rothe C, Monkman AP. J Phys Chem C 2007;111:18759.
[32] Mitsuo K, Hiroaki S, Suehiko Y. J Org Chem 1988;53:2093.
[33] Peter PF, Harvey GR. Chem Rev 1978;78:317.
[34] Yamamoto T, Morita A, Miyazaki Y, Maruyama T, Wakayama H, Zhou ZH, et al. Macromolecules 1992;25:1214.
[35] Joshi HS, Jamshidi R, Tor Y. Angew Chem Int Ed 1999;38:2721.